Topology Optimization for Orthotropic Supports in Additive Manufacturing

Matías Godoy

Topology Optimization for Orthotropic Supports in Additive Manufacturing

Matías Godoy[1]

[1]CMAP, CNRS, Ecole Polytechnique, Institut Polytechnique de Paris, 91128 Palaiseau, France. matias.godoy@cmap.polytechnique.fr

1 Introduction

In this report we study a problem which arises in the context of support structures in additive manufacturing. Support structures are used in Additive Manufacturing (AM) to ensure the quality of the final part. They are used, for example, to deal with overhanging regions when the final part cannot be self-supporting, or, to avoid deformations on the final part due to thermal residual stresses.
In the work [1] several mathematical models are proposed to deal with this issues, leading to optimization problems which are numerically computed using the level set topology optimization method [2]. In this framework, the supporting structure is assumed to be made of an *isotropic* material, this is, a material with same mechanical properties in any direction.
In this work, we consider the problem of printing a shape ω together with its supports S such that the *compliance* is minimal. The material of the shape ω is considered isotropic and the material of the supports S are considered *orthotropic*, this is, a material whose mechanical properties are different between mutually orthogonal directions. This may be a reasonable assumption in consideration as, in real manufacturing, the supports are grid structures, which could be modeled as an equivalent volume with different material properties on each direction. The studied case, following [1], is the minimization of the compliance assuming the shape ω fixed, this is, we want to determine the supports for the structure ω which has only the influence of his own weight. We explore a two dimensional reference case to study eventual qualitative differences whenever we impose stronger material properties on some directions, and we compare them also with the isotropic case.
This study is motivated as a part of the research project SOFIA (**SO**lutions pour la **F**abrication **I**ndustrielle **A**dditive metallique), whose main objective is to contribute for new developments in AM technologies.

2 Anisotropic Supports

Anisotropic materials are characterized by the fact that the material properties are different when we study their mechanical properties with respect to different directions. A subset of this materials are the orthotropic materials, which have material properties that differ along mutually-orthogonal axes of rotational symmetry. In contrast, isotropic materials have the same properties independently of the measuring direction.
We begin by exploring the involved formulations and main changes with respect with the

isotropic setting.
Given a shape ω and the supports S, both being open sets of $\mathbb{R}^d$ ($d = 2$ or $d = 3$) with ω made of an isotropic material and S made of an *orthotropic* material, such that the shape ω in this work is fixed and only the supports S are optimized. The supported structure is denoted $\Omega = S \cup \omega$ and, as usual, is assumed to be contained in a rectangular *build chamber* D. The baseplate will always be the bottom boundary of D, and is denoted $\Gamma_D := \{x \in D : x_d = 0\}$. We assume, except when mentioned, the support is clamped to the baseplate Γ_D. The other regions of the boundary of the supported structure Ω are traction free, denoted by Γ_N. In the following we consider the space, for $\Omega \subset \mathbb{R}^d$ open set, and Γ a $(d-1)$-dimensional set:

$$H^1_\Gamma(\Omega)^d := \left\{ u \in H^1(\Omega)^d : \ u = 0 \text{ on } \Gamma \right\} \tag{2.1}$$

The supported structure Ω is governed by the linearized elasticity with only gravity forces are applied to Ω. In this context, optimizing the support S for minimizing the compliance of Ω will induce minimal overhang regions. The elastic displacement u_{spt} of the supported structure $\Omega = \omega \cup S$ is the unique solution in the space $H^1_{\Gamma_D}(\Omega)$ to the mechanical system:

$$\begin{cases} -\text{div}\left(\sigma(u_{spt})\right) = \rho g & \text{in } \Omega, \\ u_{spt} = 0 & \text{on } \Gamma_D, \\ \sigma(u_{spt})n = 0 & \text{on } \Gamma_N. \end{cases} \tag{2.2}$$

Where σ is the *stress tensor* which is related with the *strain tensor* e, which in the linearized case is given by $e(u) = \dfrac{1}{2}\left(\nabla u + \nabla u^T\right)$, via the Hooke's law:

$$\sigma = Ce \tag{2.3}$$

where C is a fourth order tensor, usually called the *elasticity tensor* or simply 'Hooke law' of the material. Using the minor and major symmetries of the tensor C, due to the symmetry of the tensors σ and e, we can rewrite the relation in a vector form, using Voigt notation (see [5]), as:

$$\sigma = Ae \tag{2.4}$$

Where now A is matrix and σ, e are vectors using Voigt notation. The explicit form of C (or A) will depend on the material properties considered and in our particular case will be of special interest, as we are considering materials with different properties on each 'part' (shape or supports), this will imply in particular that we will consider (analogously for C):

$$A_\Omega = A_\omega \chi_\omega + A_S \chi_S,$$

where $\chi_{\mathcal{O}}$ is the indicator function for the set $\mathcal{O}$. This decomposition means that the mechanical properties on the fixed shape ω and the optimizable supports S, will be assumed in general different; with a *sharp-interface*.

When the considered material is *isotropic*, we can relate the quantities $\sigma(u)$ with $e(u)$ in the form:

$$\sigma(u) = Ce(u) = 2\mu e(u) + \lambda \,\text{tr}\left(e(u)\right) \text{Id} \ = 2\mu e(u) + \lambda \,\text{div}\, u \,\text{Id} \tag{2.5}$$

where μ, λ are the Lamé coefficients of the material. This will be the setting for the fixed part ω.

Remark 2.1. *The variational formulation for the system* (2.2) *in the isotropic case is:*

$$\begin{cases} \text{Find } u \in H^1_{\Gamma_D}(\Omega) \text{ such that, for any } v \in H^1_{\Gamma_D}(\Omega): \\ \displaystyle\int_\Omega 2\mu e(u)\cdot e(v)\ dx + \int_\Omega \lambda \mathrm{div}\, u \mathrm{div}\, v\ dx = \int_\Omega \rho g \cdot v\ dx \end{cases} \tag{2.6}$$

however, in anisotropic cases, we cannot expect to have such a compact formula.

How things change when the material is anisotropic? Let us focus on the orthotropic case, in which we have, in Voigt notation:

$$\begin{bmatrix} \sigma_1 \\ \sigma_2 \\ \sigma_3 \\ \sigma_4 \\ \sigma_5 \\ \sigma_6 \end{bmatrix} = \begin{bmatrix} C_{11} & C_{12} & C_{13} & 0 & 0 & 0 \\ C_{12} & C_{22} & C_{23} & 0 & 0 & 0 \\ C_{13} & C_{23} & C_{33} & 0 & 0 & 0 \\ 0 & 0 & 0 & C_{44} & 0 & 0 \\ 0 & 0 & 0 & 0 & C_{55} & 0 \\ 0 & 0 & 0 & 0 & 0 & C_{66} \end{bmatrix} \begin{bmatrix} e_1 \\ e_2 \\ e_3 \\ e_4 \\ e_5 \\ e_6 \end{bmatrix} \tag{2.7}$$

this implies, in the most general case, that the derivatives of u (and the test function v) are weighted differently in comparison of the compact formula (2.5). We will specify this quantities in the next section.

The mechanical performance of the structure Ω is measured by means of its structural compliance, given by:

$$J(S) = \int_{\omega \cup S} Ae(u_{spt})\cdot e(u_{spt})dx = \int_{\omega\cup S} \rho g \cdot u_{spt} dx\ . \tag{2.8}$$

the latter equality comes from the variational formulation of the problem taking the test function as the solution u_{spt}. It is worth notice that therefore, this quantity is (explicitly) independent of the Hooke's law considered (however is implicitly dependent of it, as u_{spt} depends of it). The admissible supports for this problem are allowed in the following set:

$$\mathcal{U}_{ad} := \{S \subset (D \setminus \omega) \text{ such that, } \Gamma_D \cap \partial S \neq \emptyset,\ \partial\omega \cap \partial S \neq \emptyset\} \tag{2.9}$$

And notice also that the objective functional, in order to avoid trivial solutions, will be

$$\mathcal{L}(S) := J(S) + \ell\ Vol(S) \tag{2.10}$$

where ℓ is a Lagrange multiplier (a penalization parameter or adjusted parameter in the optimization process).

In order to minimize (2.10) with respect to the admissible supports $\mathcal{U}_{ad}$, we rely on the concept of shape derivatives, based on the Hadamard boundary variation method (see [6]), this is: we measure the changes on the cost given by (2.10) whenever the set S is perturbed by a vector field $\theta \in W^{1,\infty}(\mathbb{R}^d, \mathbb{R}^d)$ in the sense:

$$\theta \mapsto S_\theta := (Id + \theta)(S),$$

with this, we can define the concept of shape derivative of a functional:

Definition 2.2. *A function $F : \mathcal{U}_{ad} \to \mathbb{R}$ is shape differentiable at S if the map $\theta \mapsto F(S_\theta)$ is Fréchet-differentiable at 0. The shape derivative, denoted $F'(S)$, satisfies the following asymptotic expansion:*

$$F(S_\theta) = F(S) + F'(S)(\theta) + o(\theta)$$

in a neighborhood of $0 \in W^{1,\infty}$.

Independent of the Hooke's law considered, we have the following result (which can be obtained using, for example, the formal method of Céa; see [1, 4]):

Proposition 2.3. *Assuming $\theta \cdot n = 0$ on $\partial S \cap \partial\omega$ (this is, assuming that interface between ω and S is fixed). The shape derivative of the compliance (2.8) is given by*

$$J'(S)(\theta) = \int_{\partial S \cap \omega^c} (-Ae(u_{spt}) \cdot e(u_{spt}) + 2\rho g \cdot u_{spt})\ \theta \cdot n\ ds \tag{2.11}$$

where u_{spt} is the solution of (2.2) and the compliment of ω is respect to D, and $\partial S \cap \omega^c = \partial S \setminus \partial\omega$.

Remark 2.4. *It is important to notice that this formula is valid only under the assumption that the shape ω remains fixed (which is a realistic assumption in the case when, for design reasons, we cannot change it). If we allow to optimize ω and S simultaneously, the different material properties between ω and S will impose additional terms to the shape derivative and the hypothesis $\theta \cdot n = 0$ on the interface will be no longer valid. See [1] for details for such problem.*

Remark 2.5. *Thanks to the previous propostion, we can find a descent direction θ for the cost functional $\mathcal{L}$, which is given by:*

$$\theta = -(-Ae(u_{spt}) \cdot u_{spt} + 2\rho g \cdot u_{spt} + \ell)n = -vn \tag{2.12}$$

with this, we obtain:

$$\mathcal{L}'(S)(\theta) = \int_{\partial S \cap \omega^c} -v^2 ds < 0$$

which, using the asymptotic expansion from definition 2.2, allows, for a small enough t, obtain a shape $S_{t\theta}$ with a smaller cost: $\mathcal{L}(S_{t\theta}) < \mathcal{L}(S)$.

2.1 Orthotropic material: 2d case

When we consider a 2-dimensional scenario we are saying that the case in study is a *plane strain* problem, this is, a problem where the displacement takes places only in two orthogonal directions. This is equivalent to the following definition.

Definition 2.6. *If the strain state at a material particle is such that the only non-zero strain components act in one plane only, the particle is said to be in plane strain.*

Choosing the plane XY as the plane where the strains are non-zero, we have

$$e_{xz} = e_{yz} = e_{zz} = 0 \tag{2.13}$$

So, the strain matrix becomes

$$e = \begin{bmatrix} e_{xx} & e_{xy} & 0 \\ e_{xy} & e_{yy} & 0 \\ 0 & 0 & 0 \end{bmatrix} \tag{2.14}$$

and, in this case, the Hooke's law becomes, in Voigt notation:

$$\begin{bmatrix} \sigma_{11} \\ \sigma_{22} \\ \sigma_{12} \end{bmatrix} = \begin{bmatrix} 2\mu_1 + \lambda & \lambda & 0 \\ \lambda & 2\mu_2 + \lambda & 0 \\ 0 & 0 & \gamma \end{bmatrix} \begin{bmatrix} e_{11} \\ e_{22} \\ 2e_{12} \end{bmatrix} \tag{2.15}$$

In principle λ should also be different on each direction, however for sake of simplicity we let it constant as for testing purposes will be enough considering different Young modulus. The variational formulation of (2.2), if we assume that the whole material in Ω is orthotropic, becomes:

$$\begin{cases} \text{Find } u \in H^1_{\Gamma_D}(\Omega) \text{ such that, for all } v \in H^1_{\Gamma_D}(\Omega): \\ \int_\Omega 2\mu_1 \partial_1 u_1 \partial_1 v_1 + \lambda(\partial_1 u_1 + \partial_2 u_2)(\partial_1 v_1 + \partial_2 v_2)\ dx \\ + \int_\Omega 2\mu_2 \partial_2 u_2 \partial_2 v_2 + \gamma(\partial_2 u_1 + \partial_1 u_2)(\partial_1 v_2 + \partial_2 v_1)\ dx \\ = \int_\Omega \rho g \cdot v\ dx \end{cases} \tag{2.16}$$

For our computations, we consider, instead of Lamé coefficients λ, μ, the Young modulus E_i and the Poisson ratio ν (this latter one fixed to 0.3). The coefficients are related in the following way (in the isotropic case)

$$\mu = \frac{E}{2(1+\nu)}, \lambda = \frac{E\nu}{(1+\nu)(1-2\nu)}$$

in our simplified case we will consider:

$$\mu_i = \frac{E_i}{2(1+\nu)},\ \lambda = \frac{E_\omega \nu}{(1+\nu)(1-2\nu)}$$

where E_ω stands for the fixed part ω Young's modulus and E_1 and E_2 will be the Young's modulus on horizontal ($i = 1$) and vertical ($i = 2$) directions for the support S, this will be (roughly) a measure of the strength of the support S on each direction.

2.2 The level-set method for shape optimization

The level-set method has been proposed by Osher and Sethian (see [10]) for tracking fronts and free boundaries, it is used for several applications in image processing, fluid mechanics, etc. In structural optimization it has been proposed as a powerful tool by Allaire, Jouve and Toader (see [2]) which allows to perform shape and topological optimization in this context with a less computational cost (avoiding unnecessary remeshing).
In this context, let us consider a computational working domain $D \subset \mathbb{R}^d$ in which all admissible shapes S are included and such that the loaded boundaries Γ_D, Γ_N are included in ∂D. The mesh on D is fixed and the shape S of the actual support is implicitly defined by a level set function ϕ, defined on D, by:

$$\begin{cases} \phi(x) < 0 \Leftrightarrow x \in S \\ \phi(x) = 0 \Leftarrow x \in \partial S \cap D \\ \phi(x) > 0 \Leftrightarrow x \in D \setminus S \end{cases}$$

As we are interested to compute the shape derivative $J'(S)(\theta)$ given by (2.11), we need to compute the solution of the system (2.2), however as Ω is implicitly defined by the level set function, no mesh is available to solve it. In order to overcome this problem, we consider the *Ersatz approach*, which consists on filling the the complementary part $D \setminus (S \cup \omega)$ with a with a very soft material with Hooke's tensor εA with $\varepsilon \ll 1$ (typically $\varepsilon = 10^{-3}$), and therefore we solve the problem, defined on the whole computational domain D:

$$\begin{cases} -\text{div}\,(A_\varepsilon e(u_{spt})) = \rho g & \text{in } D, \\ u_{spt} = 0 & \text{on } \Gamma_D, \\ \sigma(u_{spt}) n = 0 & \text{on } \Gamma_N, \end{cases} \tag{2.17}$$

with $A_\varepsilon(x) := \begin{cases} A = A_\omega \chi_\omega + A_S \chi_S & \text{if } x \in \Omega \\ \varepsilon A_\omega & \text{if } x \in D \setminus \Omega. \end{cases}$
This method is proved to be consistent (see [3]).

In order to track the evolution of the shape S as we perform the minimization of the cost functional $\mathcal{L}$, we have to relate the movement of the level-set function ϕ for S^{k-1} (the shape of the supports at the $(k-1)$ iteration of the numerical algorithm) and the normal velocity $\theta = -vn$ given by (2.12), which ensures that the new shape $S^k := S^{k-1}_{t\theta}$ is such that $\mathcal{L}(S^k) < \mathcal{L}(S^{k-1})$. So, as we want to transport the level set function ϕ along the gradient flow $\theta = -vn$, we have to solve the following linear transport equation (introducing a time variable for the step t):

$$\partial_t \phi + \theta \cdot \nabla \phi = 0 \text{ on } [0, \tau] \times D$$

which, for the given θ, provides the Hamilton-Jacobi equation:

$$\partial_t \phi - v \|\nabla \phi\| = 0 \text{ on } [0, \tau] \times D \tag{2.18}$$

with initial condition $\phi(0, x)$ taken as the input level set (without time). The new level set will correspond to $\phi(\tau, x)$.

Finally, it is important to notice that, in order to solve the equation (2.18) we need to have a field θ defined on the whole box D, instead of the expression (2.12) deduced from the shape derivative (2.11) which is defined only on $\partial S \cap \omega^c$. To this end, following [7] we perform a process called *extension-regularization* of the velocity, solving the problem:

$$\begin{cases} \text{Find } Q \in H^1(\mathbb{R}^d) \text{ such that:} \\ \displaystyle\int_D \alpha_{reg}^2 \nabla Q \cdot \nabla v + Q \cdot v \; dx = \mathcal{L}'(\Gamma)(vn) \; \forall v \in H^1(\mathbb{R}^d) \end{cases} \tag{2.19}$$

where the parameter α_{reg} is the minimal element size from the mesh of D.

We can resume the procedure in the following algorithm:

Algorithm 1 Shape optimization of an orthotropic support structure for a fixed part minimizing the compliance

Require: S^0, a given support structure and its level set function ϕ_0; ω the fixed part.
  while $k \leq k_{maxiter}$ **do**
    Solve elasticity system on $\Omega^k = S^k \cup \omega$.
    Compute the normal velocity (descent direction) v^k using formula (2.12) and solving the extension-regularization problem (2.19).
    Put $t = initial\_step$
    while $j \leq j_{max}$ (Loop for Line search) **do**
      Let $\phi_j^k := \phi^k$.
      Transport ϕ^k solving (2.18) with $\theta = -v^k n$ using $\tau = t$.
      Compute Hooke's tensor A^k associated with the transported ϕ^k.
      if $\mathcal{L}(\Omega_{t\theta}^k) < (1 + tol)\mathcal{L}(\Omega^{k-1})$ **then**
        $\phi^k \leftarrow Transport(\phi^k)$
        break
      else
        $\phi^k \leftarrow \phi_j^k$ (Undo the transport).
        $t \leftarrow \max(0.5t, t_{min})$
      end if
      $j \leftarrow j + 1$
    end while
    New shape is defined by $\{x \in D : \ \phi^k(x) < 0\}$.
    Update parameters (augmented Lagrangian case)
    $k \leftarrow k + 1$
  end while

2.3 Numerical Testing

In the following, we consider a few tests in order to study how much a solution changes when the horizontal-vertical properties (the Young modulus E_i) changes in the orthotropic cases with respect with the isotropic case: $E_1 = E_2$. We present two different geometries with several initialization procedures, recalling that, in general, we are obtaining local minima. For simplicity we take, in all the simulations, $\nu = 0.3$, $\gamma = \dfrac{\mu_1 + \mu_2}{2}$ and then we will test how behaves the structure when the Young modulus of the supports changes (this is, we only modify E_1, E_2 or, equivalently, μ_1, μ_2; where the index 1 is related to horizontal strength and 2 is related to vertical strength).
All the simulations are performed using the Finite Element software *FreeFEM++* (see [8]), the transport of the level set is performed using the package *Advect* [9].

2.3.1 The diagonal shape

In this case the geometry of the fixed part to be supported is a diagonal bar, with homogeneous Dirichlet boundary condition at the bottom and rightside of the domain $D = [0, 1] \times [0, 1]$, the rest have an homogeneous Neumann boundary condition.

We consider two level set initializations, both of them are basically the domain D covered by the support material with holes distributed with different symmetries:

- Case 1:

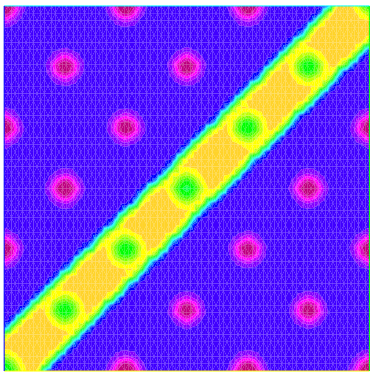

Figure 1: Initial level set function

For this configuration, we obtain the following final distribution of supports and convergence curves (volume and cost functional):

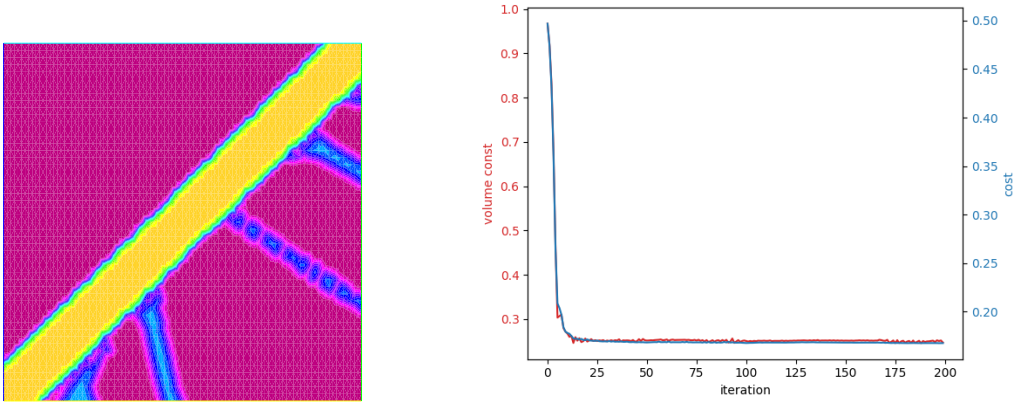

Figure 2: Anisotropic case: $E_1 = 1.0, E_2 = 0.1$

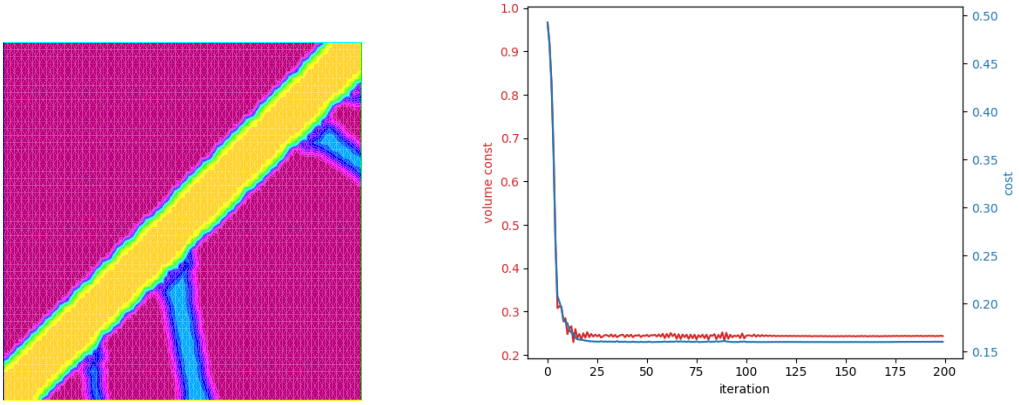

Figure 3: Anisotropic case: $E_1 = 0.1, E_2 = 1.0$

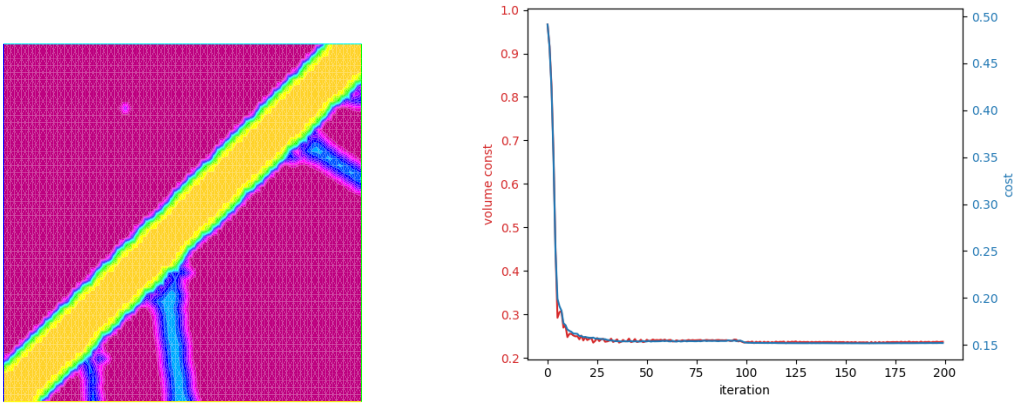

Figure 4: Isotropic case: $E_1 = E_2 = 1.0$

- Case 2:

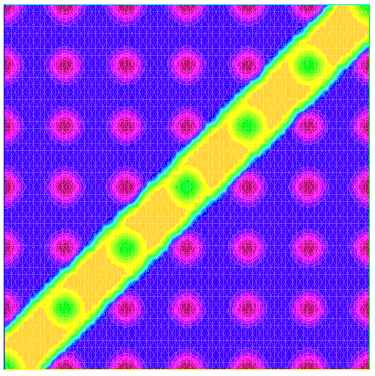

Figure 5: Initial level set function

For this configuration, we obtain the following final distribution of supports and convergence curves (volume and cost functional):

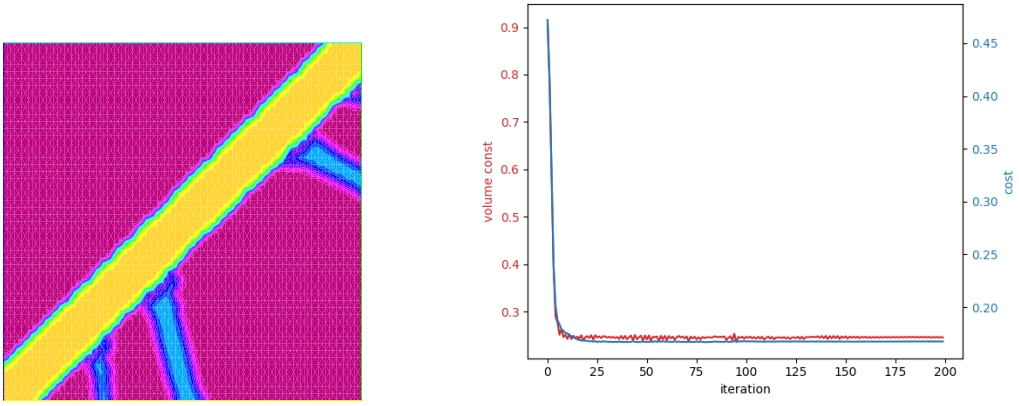

Figure 6: Anisotropic case: $E_1 = 1.0, E_2 = 0.1$

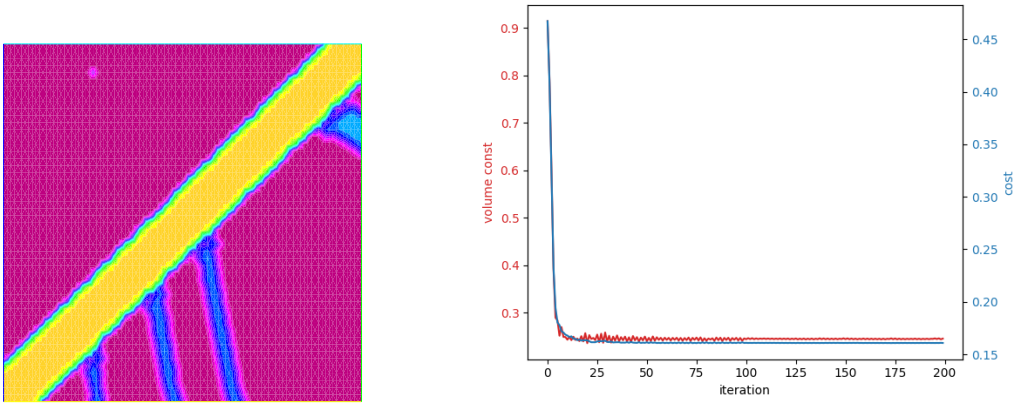

Figure 7: Anisotropic case: $E_1 = 0.1, E_2 = 1.0$

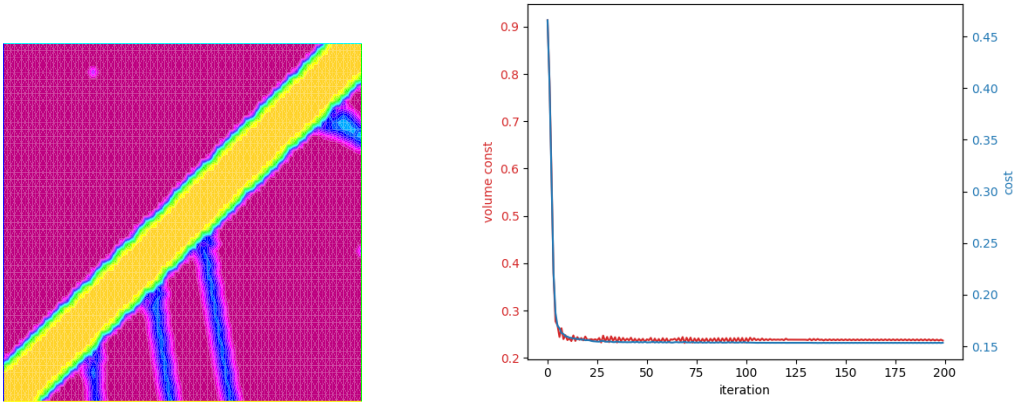

Figure 8: Isotropic case: $E_1 = E_2 = 1.0$

2.3.2 The L shape

In this case the geometry of the fixed part to be supported is an L shape with homogeneous Dirichlet boundary condition at the bottom of the domain $D = [0, 1] \times [0, 1]$, the rest of the boundary have an homogeneous Neumann boundary condition.

- Case 1:

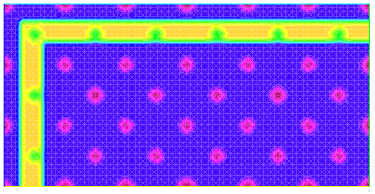

Figure 9: Initial level set function

For this configuration, we obtain the following final distribution of supports and convergence curves (volume and cost functional):

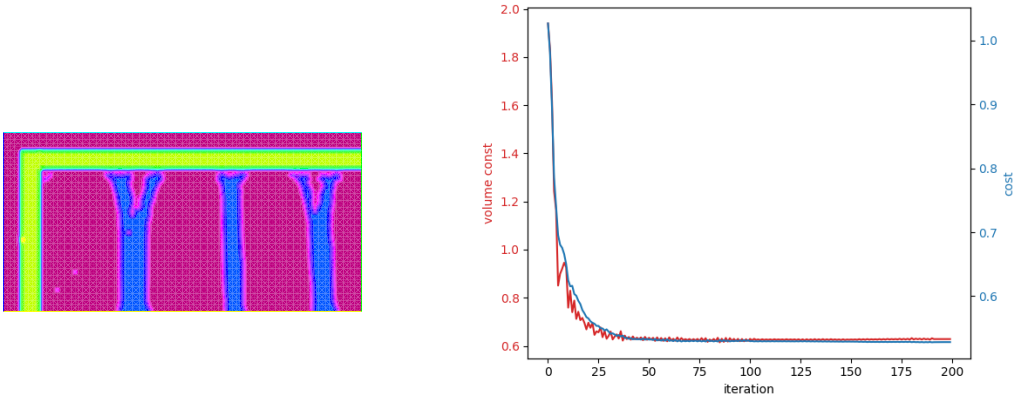

Figure 10: Anisotropic case: $E_1 = 1.0, E_2 = 0.1$

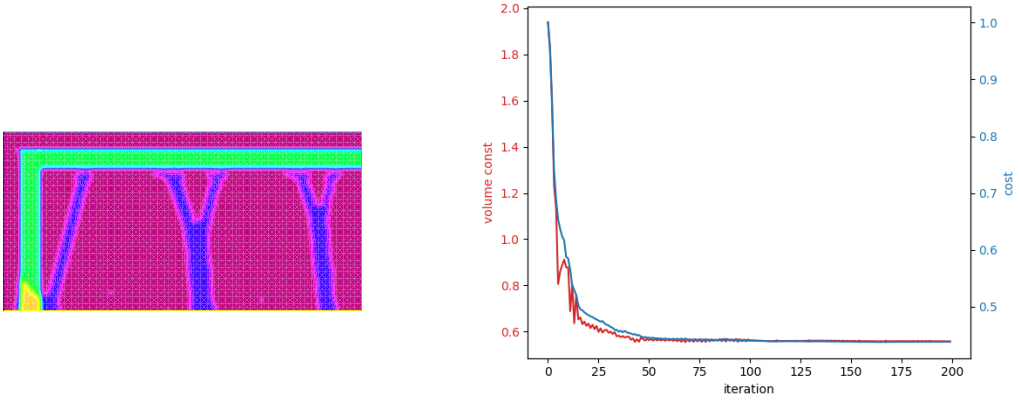

Figure 11: Anisotropic case: $E_1 = 0.1, E_2 = 1.0$

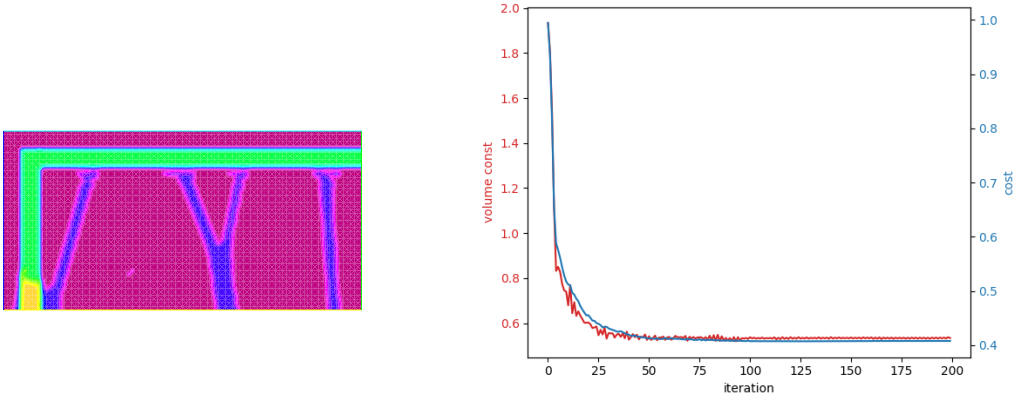

Figure 12: Isotropic case: $E_1 = E_2 = 1.0$

- Case 2:

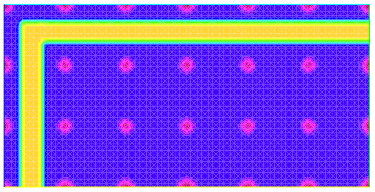

Figure 13: Initial level set function

For this configuration, we obtain the following final distribution of supports and convergence curves (volume and cost functional):

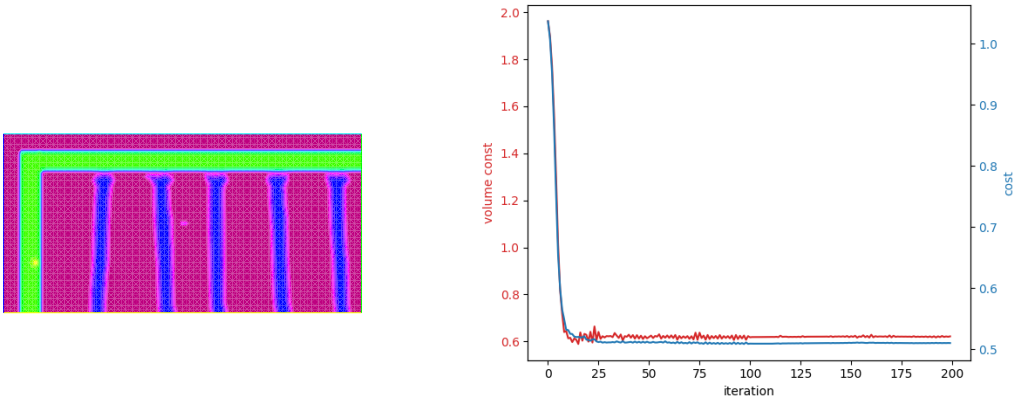

Figure 14: Anisotropic case: $E_1 = 1.0, E_2 = 0.1$

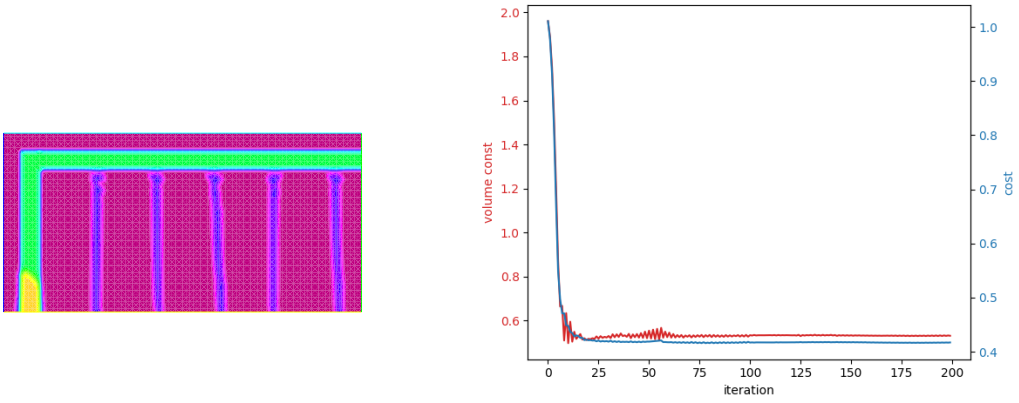

Figure 15: Anisotropic case: $E_1 = 0.1, E_2 = 1.0$

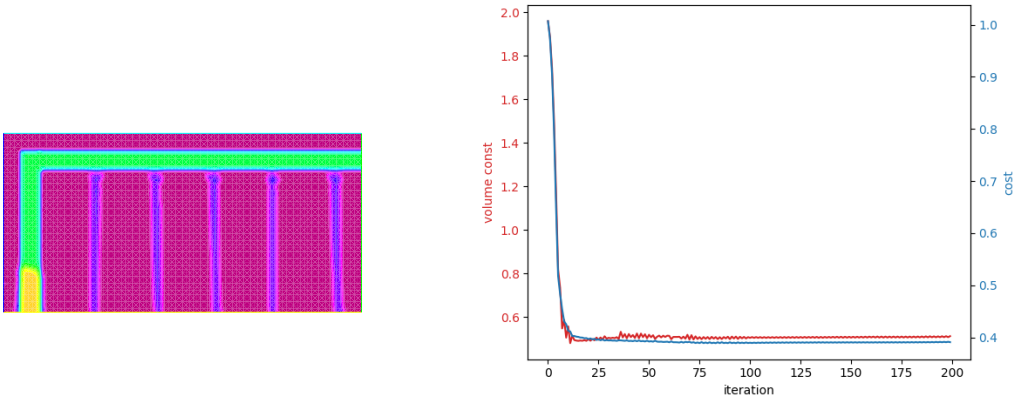

Figure 16: Isotropic case: $E_1 = E_2 = 1.0$

In this first series of examples we can observe some common behavior:

- The lowest value of the cost functional is reached on the isotropic case.
- Qualitatively, isotropic and 'vertically stronger' ($E_2 > E_1$) cases have similar topology. 'Horizontally stronger' case obtains the highest cost and their topology is different.
- As we have mentioned before, the optimal shape could be different if the initialization is different, as we can see on the L shape case.
- The reinforced zones tends to be similar in all cases, even when qualitatively the shapes for the supports are different.

2.3.3 The diagonal shape: Augmented Lagrangian

In the following, we will test the diagonal shape, now using an Augmented Lagrangian method for the optimization, this allows to impose a fixed objective volume for the supports, considering *merit* function to be optimized:

$$\mathcal{L}(\Omega, \lambda, \mu) := J(\Omega) - \lambda(Vol(\Omega) - V_{obj}) + \frac{\mu}{2}(Vol(\Omega) - V_{obj})^2$$

where V_{obj} is the objective volume and the coefficient λ is expected to converge to the Lagrange multiplier of the restriction $V = V_{obj}$. In order to do this, the theory (see [11]), suggest to update λ_{k+1} as:

$$\lambda_{k+1} = \lambda_k - \mu_k(Vol(\Omega) - V_{obj}),$$

is important to notice that, in this case, it is not necessary to take a sequence of μ_k such that $\mu_k \to +\infty$. In our examples we begin with $\mu = 0.1$ and update each 3 iterations as $\mu \leftarrow 1.3\mu$ while $\mu \leq \mu_{max} = 10.0$. We take in this examples:

$$\lambda_0 = -0.2,\ \lambda_0 = -\frac{1}{|\partial S \cap \omega^c|}\int_{\partial S \cap \omega^c} Ae(u) : e(u)\ ds;\ \mu_0 = \frac{|\lambda_0|}{2}.$$

We take the same configuration as before, imposing that the volume of the supports should be 10% of the volume of the shape in the first 3 cases, then 30% in the following 3 cases and finally 50% in the last 3 cases.

- Case 1:

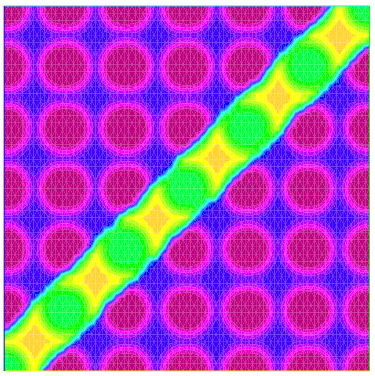

Figure 17: Initial level set function

For this configuration, we obtain the following final distribution of supports and convergence curves (volume and cost functional):

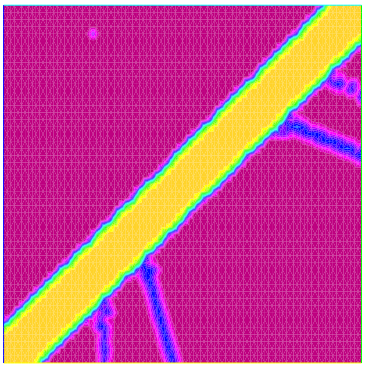

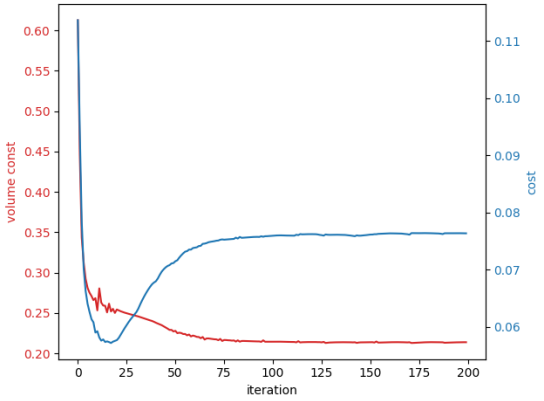

Figure 18: Anisotropic case: $E_1 = 1.0, E_2 = 0.1$

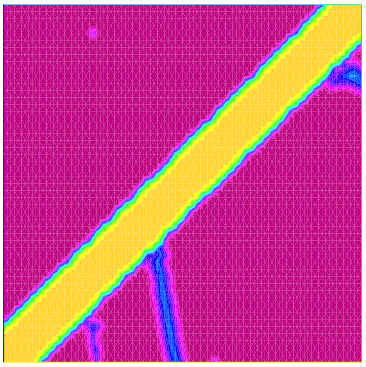

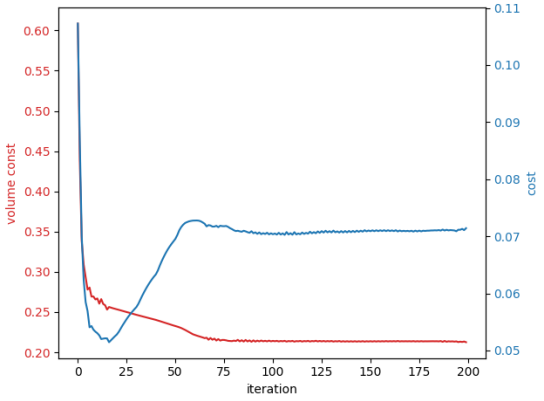

Figure 19: Anisotropic case: $E_1 = 0.1, E_2 = 1.0$

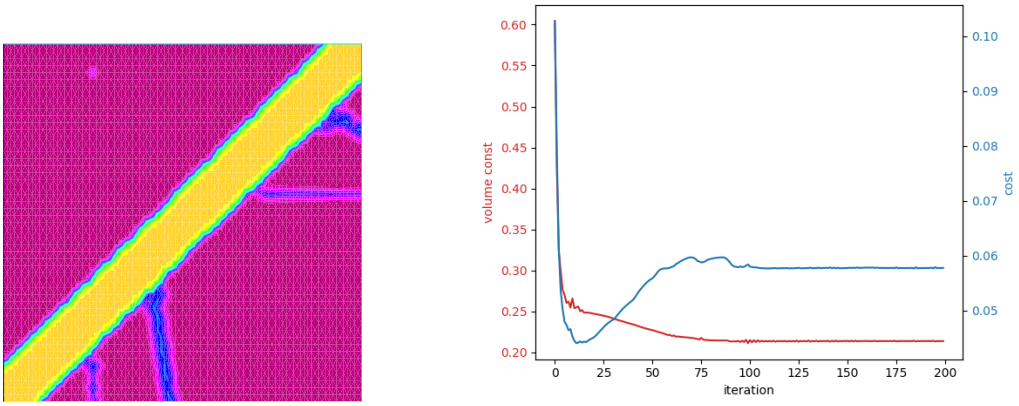

Figure 20: Isotropic case: $E_1 = E_2 = 1.0$

- Case 2:

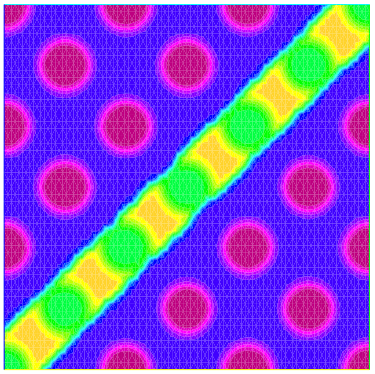

Figure 21: Initial level set function

For this configuration, we obtain the following final distribution of supports and convergence curves (volume and cost functional):

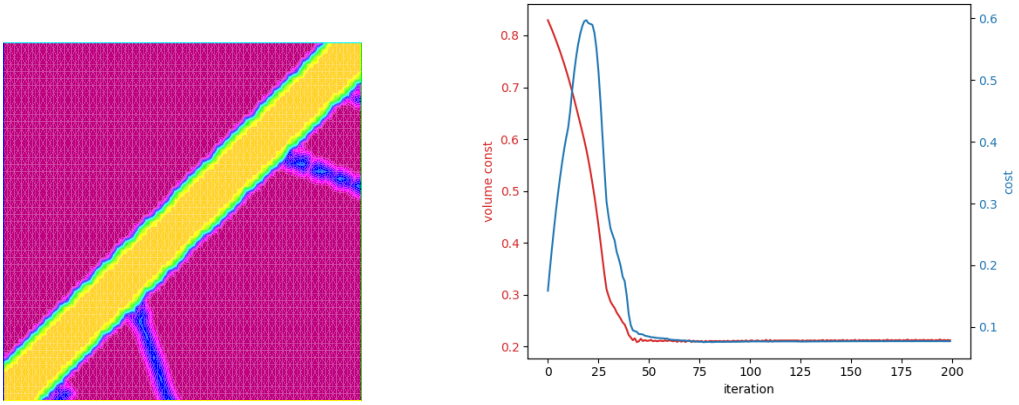

Figure 22: Anisotropic case: $E_1 = 1.0, E_2 = 0.1$

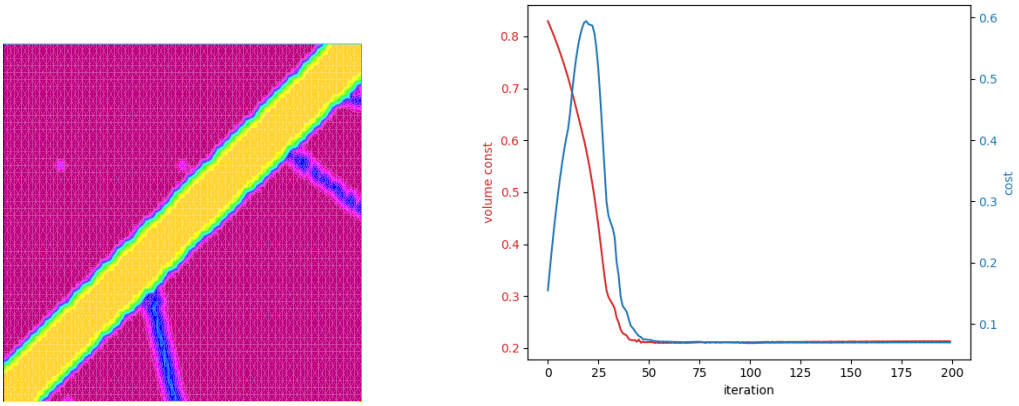

Figure 23: Anisotropic case: $E_1 = 0.1, E_2 = 1.0$

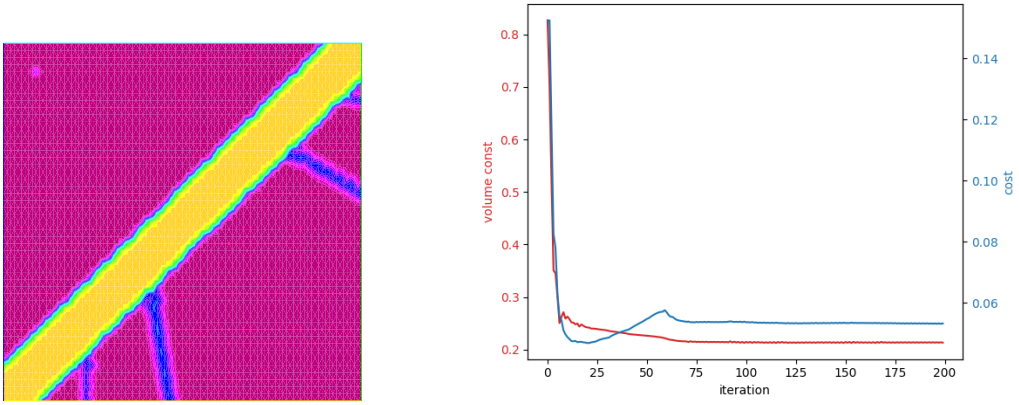

Figure 24: Isotropic case: $E_1 = E_2 = 1.0$

- Case 3:

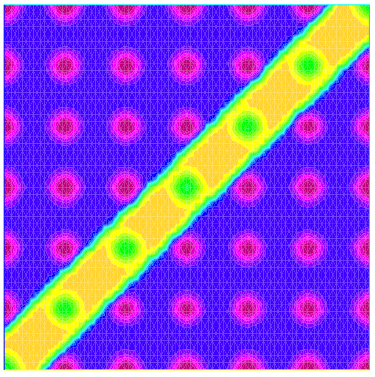

Figure 25: Initial level set function

For this configuration, we obtain the following final distribution of supports and convergence curves (volume and cost functional):

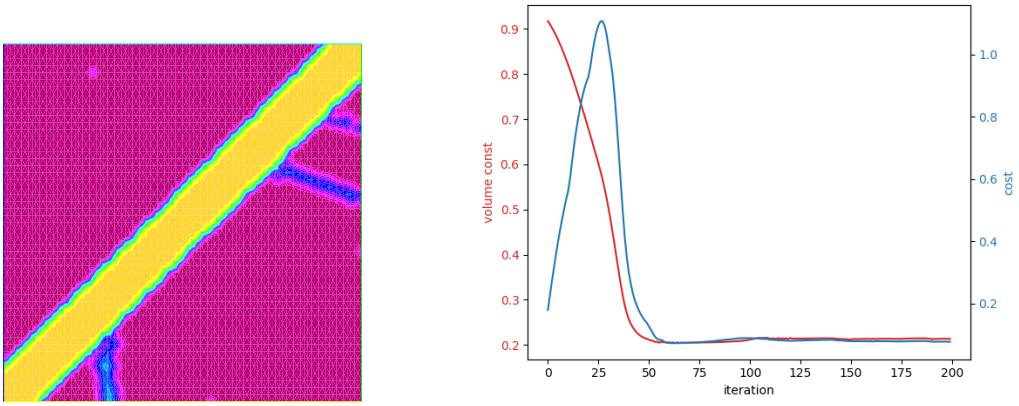

Figure 26: Anisotropic case: $E_1 = 1.0, E_2 = 0.1$

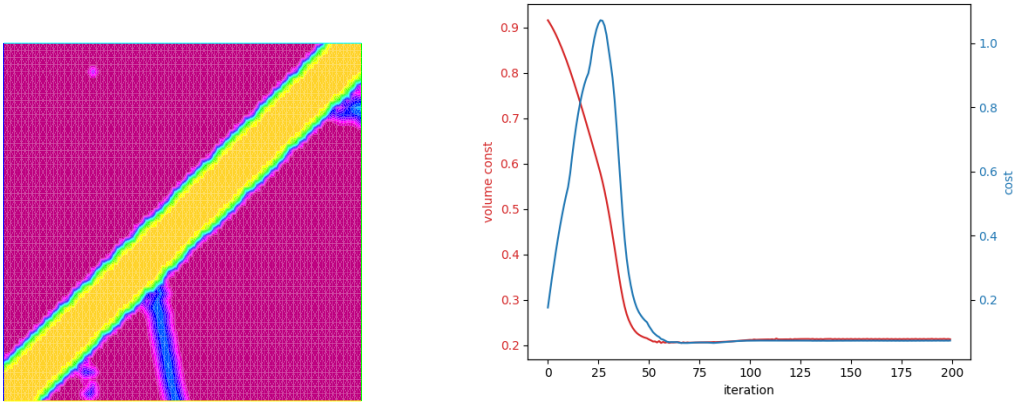

Figure 27: Anisotropic case: $E_1 = 0.1, E_2 = 1.0$

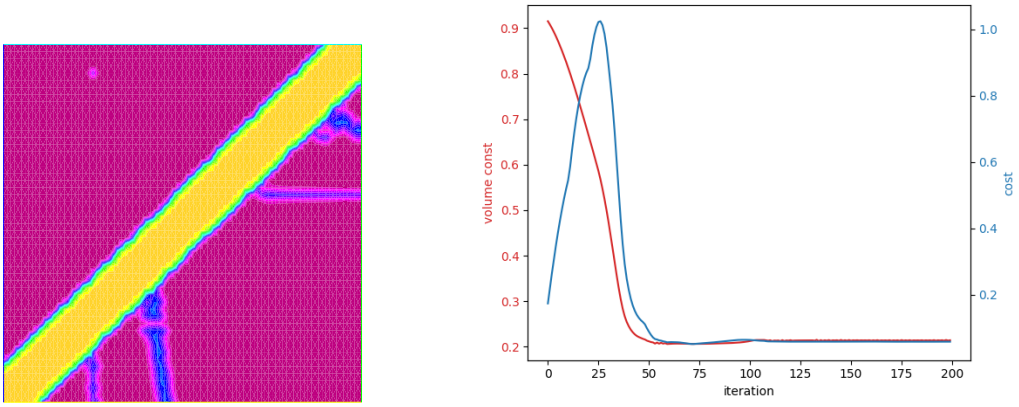

Figure 28: Isotropic case: $E_1 = E_2 = 1.0$

Remark: in the following three cases we have $V_{obj} = 1.3 \cdot V_{fixed}$.

- Case 4:

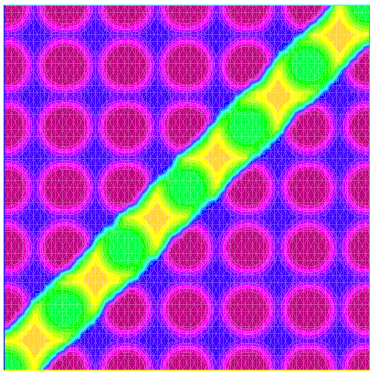

Figure 29: Initial level set function

For this configuration, we obtain the following final distribution of supports and convergence curves (volume and cost functional):

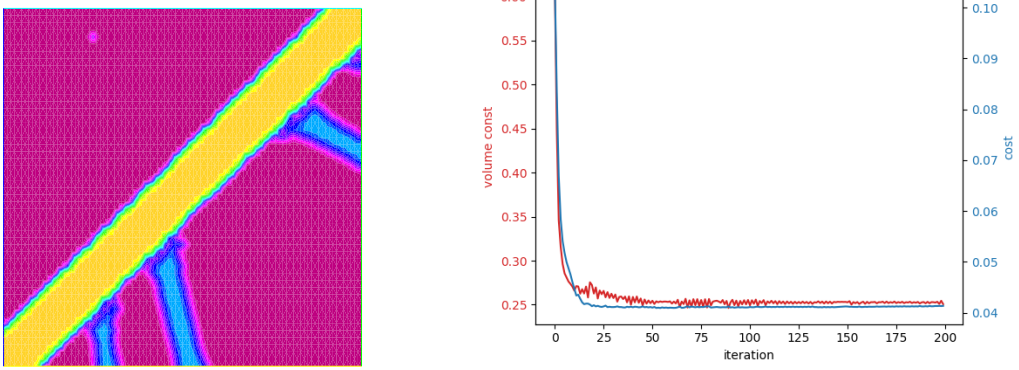

Figure 30: Anisotropic case: $E_1 = 1.0, E_2 = 0.1$

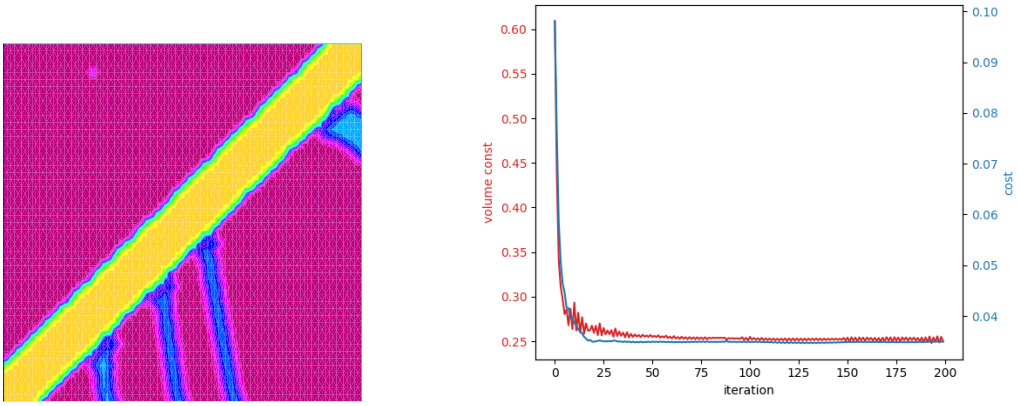

Figure 31: Anisotropic case: $E_1 = 0.1, E_2 = 1.0$

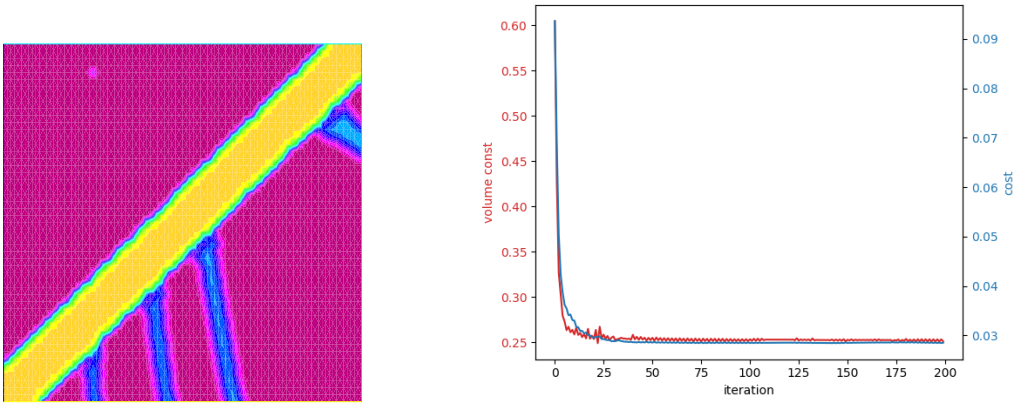

Figure 32: Isotropic case: $E_1 = E_2 = 1.0$

- Case 5:

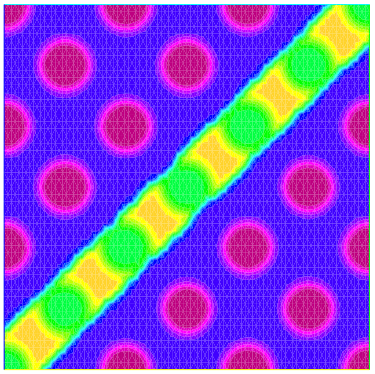

Figure 33: Initial level set function

For this configuration, we obtain the following final distribution of supports and convergence curves (volume and cost functional):

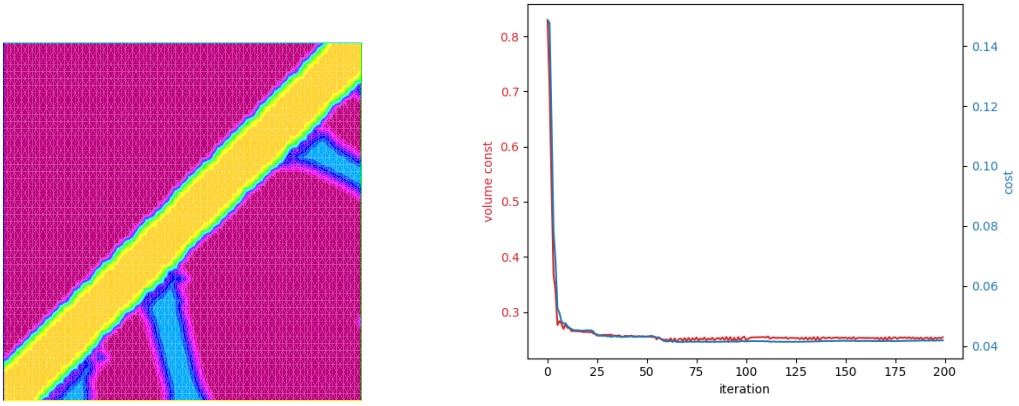

Figure 34: Anisotropic case: $E_1 = 1.0, E_2 = 0.1$

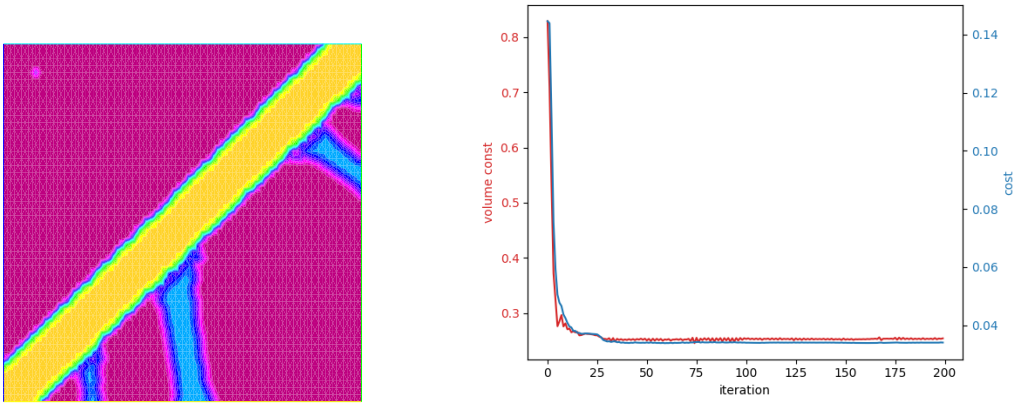

Figure 35: Anisotropic case: $E_1 = 0.1, E_2 = 1.0$

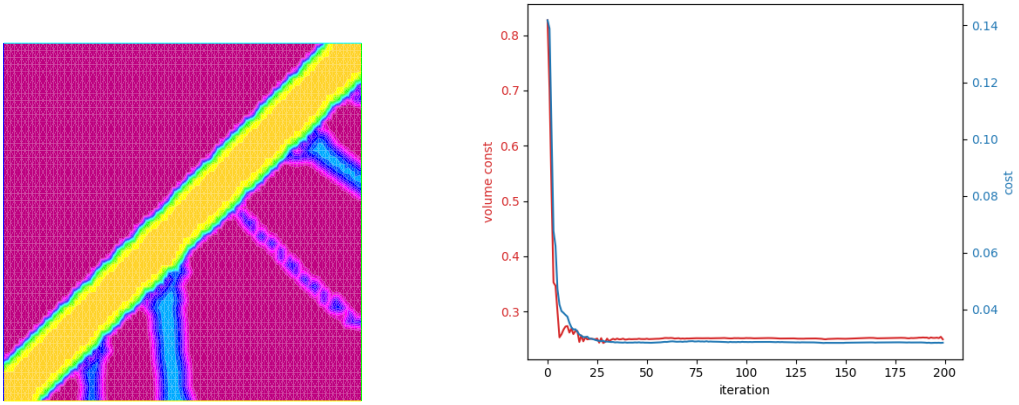

Figure 36: Isotropic case: $E_1 = E_2 = 1.0$

- Case 6:

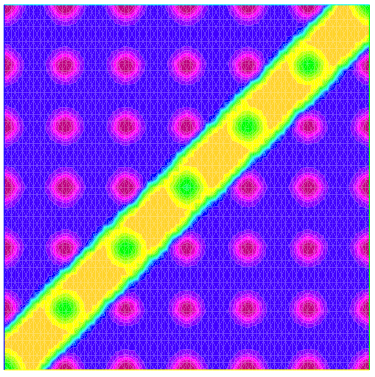

Figure 37: Initial level set function

For this configuration, we obtain the following final distribution of supports and convergence curves (volume and cost functional):

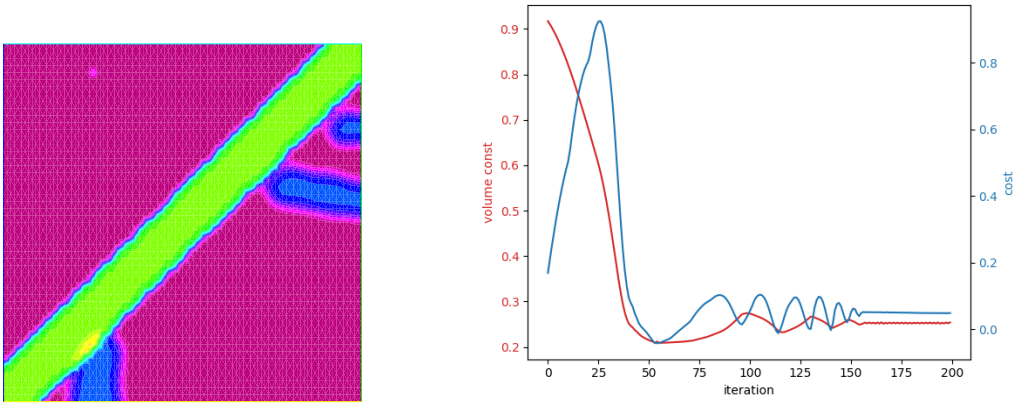

Figure 38: Anisotropic case: $E_1 = 1.0, E_2 = 0.1$

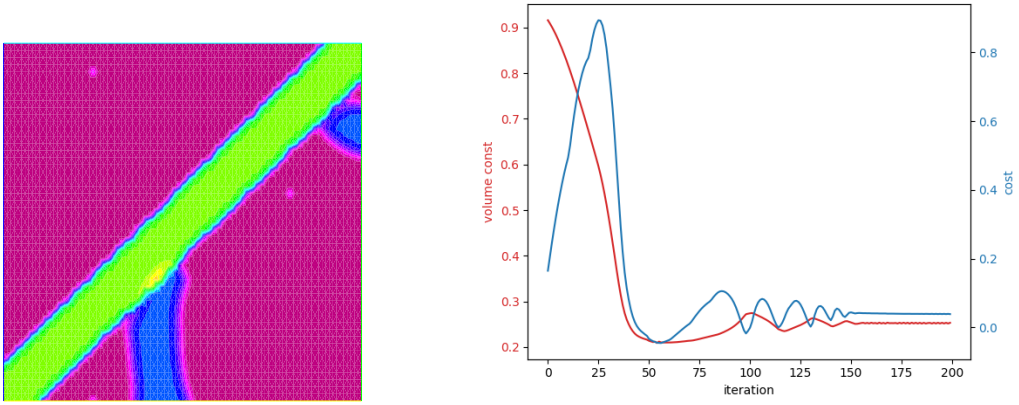

Figure 39: Anisotropic case: $E_1 = 0.1, E_2 = 1.0$

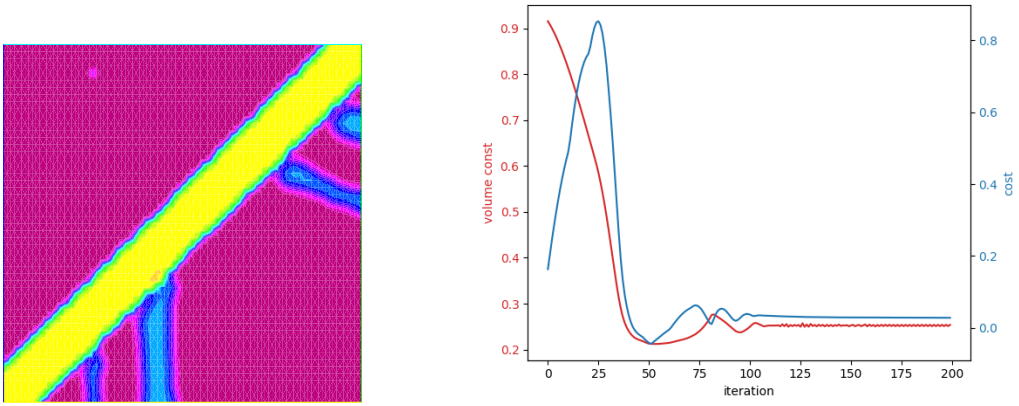

Figure 40: Isotropic case: $E_1 = E_2 = 1.0$

Remark: in the following three cases we have $V_{obj} = 1.5 \cdot V_{fixed}$.

- Case 7:

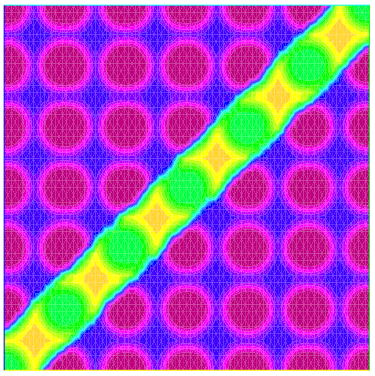

Figure 41: Initial level set function

For this configuration, we obtain the following final distribution of supports and convergence curves (volume and cost functional):

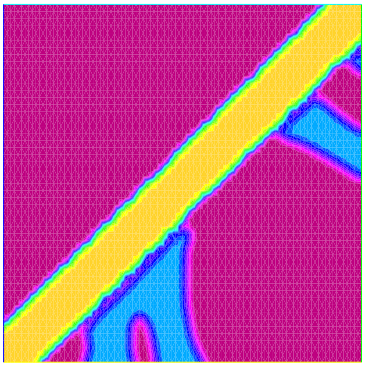

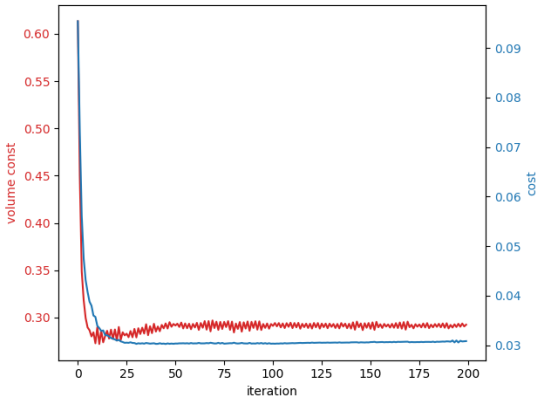

Figure 42: Anisotropic case: $E_1 = 1.0, E_2 = 0.1$

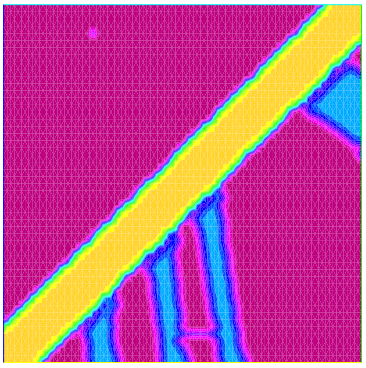

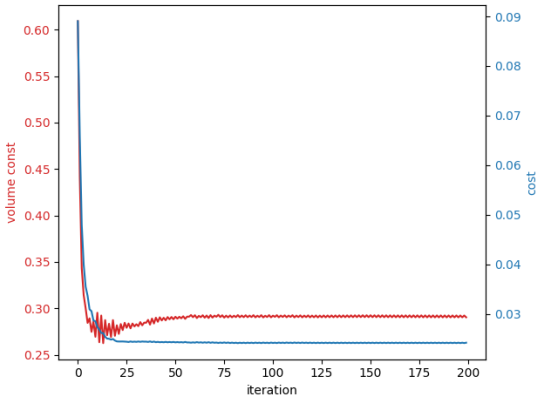

Figure 43: Anisotropic case: $E_1 = 0.1, E_2 = 1.0$

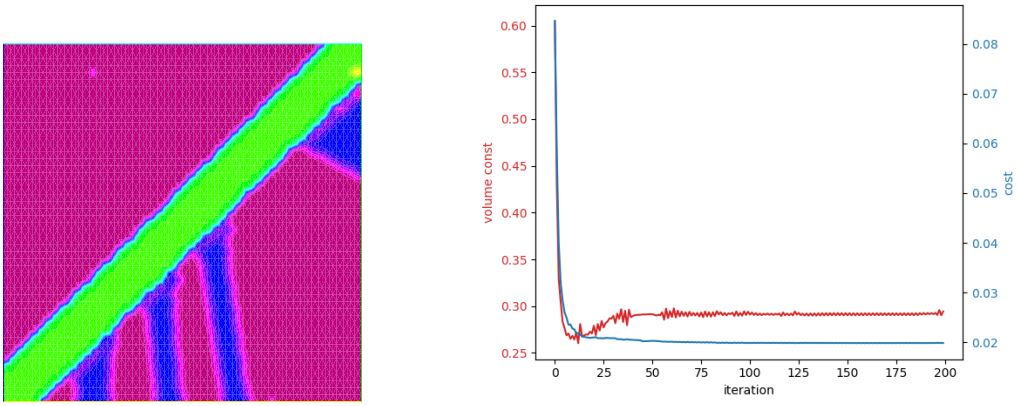

Figure 44: Isotropic case: $E_1 = E_2 = 1.0$

- Case 8:

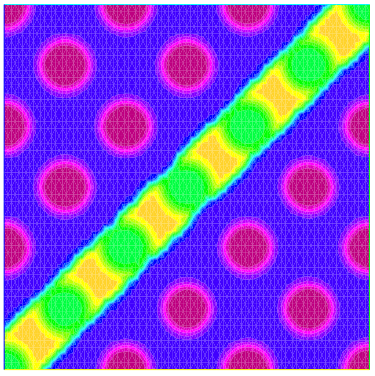

Figure 45: Initial level set function

For this configuration, we obtain the following final distribution of supports and convergence curves (volume and cost functional):

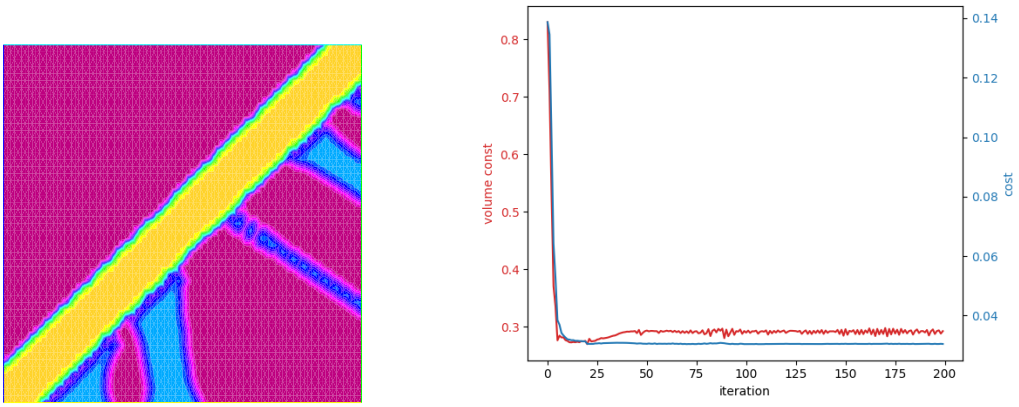

Figure 46: Anisotropic case: $E_1 = 1.0, E_2 = 0.1$

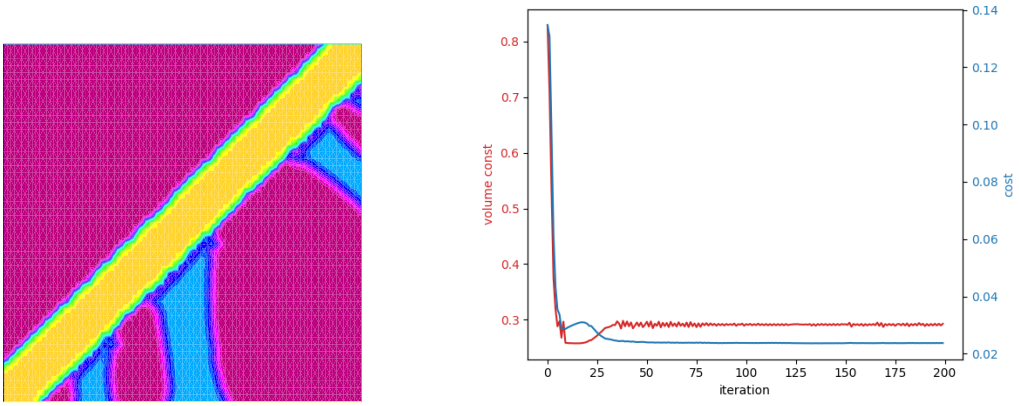

Figure 47: Anisotropic case: $E_1 = 0.1, E_2 = 1.0$

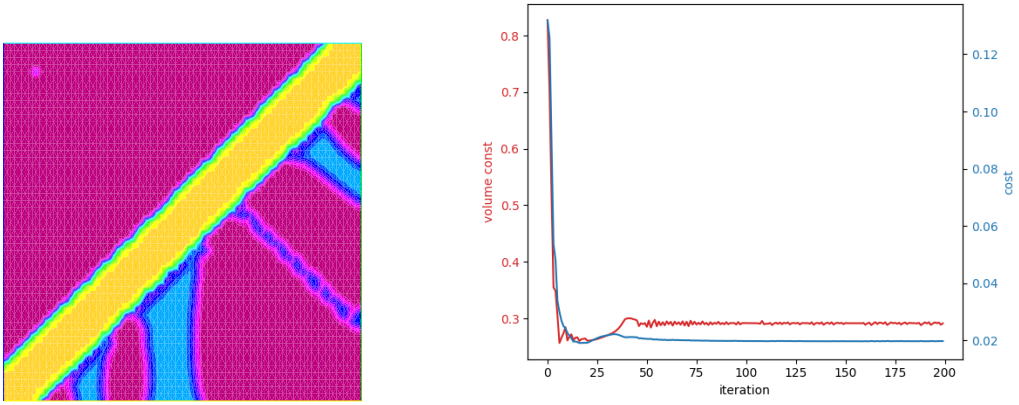

Figure 48: Isotropic case: $E_1 = E_2 = 1.0$

- Case 9:

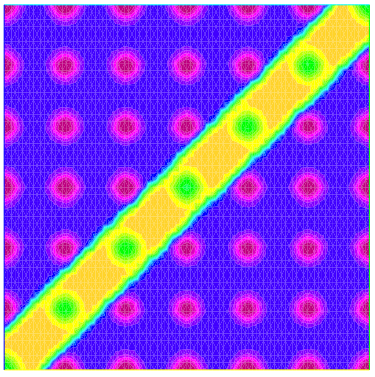

Figure 49: Initial level set function

For this configuration, we obtain the following final distribution of supports and convergence curves (volume and cost functional):

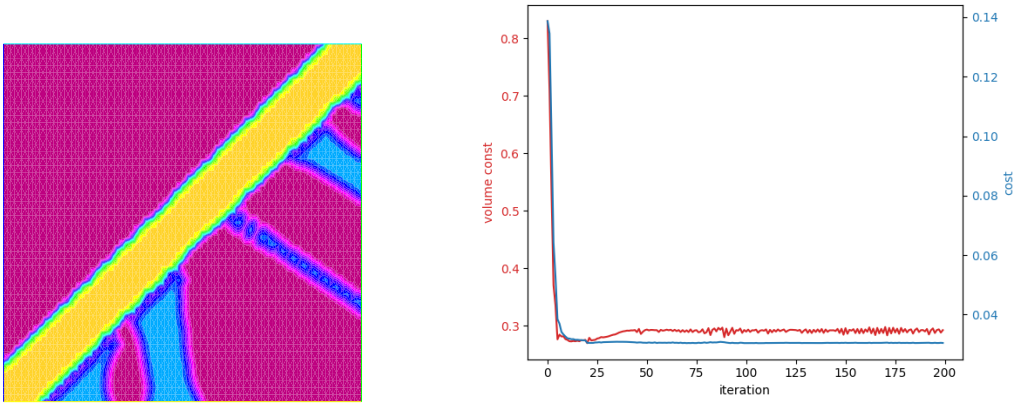

Figure 50: Anisotropic case: $E_1 = 1.0, E_2 = 0.1$

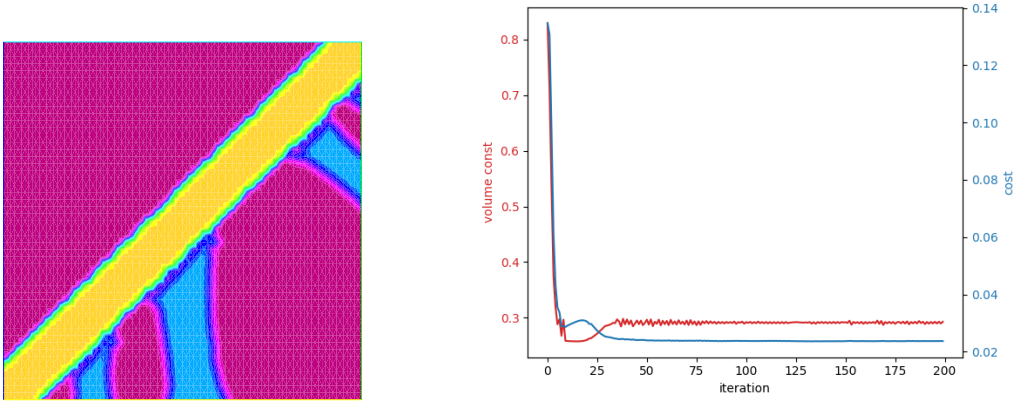

Figure 51: Anisotropic case: $E_1 = 0.1, E_2 = 1.0$

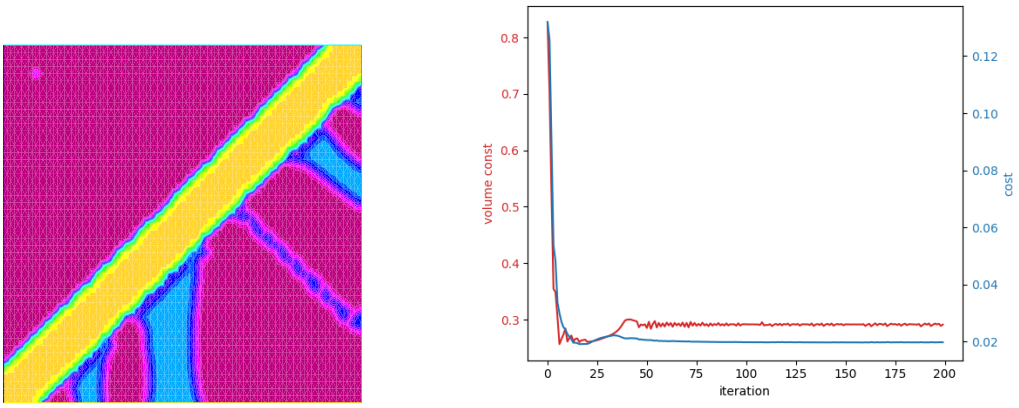

Figure 52: Isotropic case: $E_1 = E_2 = 1.0$

From this cases we can notice:

- As before, best performance is obtained on isotropic cases.
- As expected, highest target volume implies better performance.

- We obtain more variety of final configurations, with in some cases different number of connected components in all cases, however, qualitatively there are not remarkable differences.

3 Conclusions

From the performed tests we can conclude that:

- For the considered problem, the best performance is obtained with an isotropic configuration of the mechanical properties for the supports. Between horizontally or vertically stronger configurations, vertically ones perform better in all the considered tests, but however, in general the obtained configurations are not notoriously different with respect to the isotropic case.
- The zones to be supported seems to be independent of the initial topology and of the mechanical properties of the support.
- As expected, as more material we allow for the supports, the better performance we obtain.

Finally, we consider that more general models of anisotropy should be considered in order to study the possibilities on improving the performance of the supports, orthotropy is a particular case of anisotropy as well as the consideration of only the vertical and horizontal axis as the axis of orthotropy is a strong restriction.

Acknowledgements

The author wish to thank professors G. Allaire and B. Bogosel for their supervision and guidance in the development of this manuscript.
This work was partially supported by the SOFIA project, funded by BPI (Banque Publique d'Investissement).

References

[1] Allaire, G. and Bogosel, B. Optimizing supports for additive manufacturing. *Struct. Multidiscip. Optim.* (2018) **58(6)**:2493–2515.

[2] Allaire, G., Jouve, F., and Toader, A. M. A level-set method for shape optimization. *Comptes Rendus Mathematique* (2002), **334(12)**, 1125-1130.

[3] Allaire, G. Shape optimization by the homogenization method, *Springer Verlag, New York* (2002)

[4] Céa, J. Conception optimale ou identification de formes, calcul rapide de la dérivée directionnelle de la fonction cout. *ESAIM: Mathematical Modelling and Numerical Analysis* **20(3)** (1986): 371-402.

[5] Zienkiewicz, O.C. and Taylor, R. L. and Zhu, J.Z. The finite element method: its basis and fundamentals. *Butterworth-Heinemann.* (2005).

[6] Henrot, A. and Pierre, M. Variation et optimisation de formes: une analyse géométrique *Springer Science & Business Media.* (2006)

[7] de Gournay, F. Velocity extension for the level-set method and multiple eigenvalues in shape optimization. *SIAM J. on Control and Optim.*, **45(1)** (2006), 343–367.

[8] Hecht, F. New development in FreeFem++. *Journal of numerical mathematics* (2012) **20(3-4)** 251–266.

[9] C. Bui, C. Dapogny, and P. Frey. An accurate anisotropic adaptation method for solving the level set advection equation. *Internat. J. Numer. Methods Fluids*, **70(7)** (2012) 899–922.

[10] Osher, S., and Sethian, J. A. Fronts propagating with curvature-dependent speed: algorithms based on Hamilton-Jacobi formulations. *Journal of Computational Physics*, **79(1)** (1988), 12–49.

[11] Nocedal, J. and Wright, S. Numerical optimization. *Springer Science* (2006).